An apertureless near-field scanning optical microscope for imaging surface plasmons in the mid-wave infrared

John Kohoutek, Dibyendu Dey, Ryan Gelfand, Alireza Bonakdar, Hooman Mohseni

Bio-Inspired Sensors and Optoelectronics Laboratory (BISOL), EECS, Northwestern University, 2145 Sheridan Rd., Evanston, Illinois, USA

ABSTRACT

An apertureless near-field scanning optical microscope (a-NSOM) setup is described. Special consideration is given to important system components. Surface plasmons are defined, as is their relationship to a-NSOM and their interaction with the scanning probe tip. We used this set-up to measure a metal-dielectric-metal (MDM) antenna integrated with a quantum cascade laser (QCL). The former is introduced and described. The role of the atomic force microscope (AFM) in the experiment is laid out and explained. Finally, the lock-in amplifier is explained. Next, the system setup is introduced and explained from the point of view of the light path taken by light generated in the laser. Finally, results are given for the MDM single nanorod antenna and the coupled MDM nanorod antenna. Simulation, topography, and NSOM images are shown. Lastly, several experimental issues are discussed as well as other types of NSOM.

1. INTRODUCTION

A surface plasmon (SP) is a collective motion of electrons generated by light at the interface between two mediums of opposite signs of dielectric susceptibility (e.g. metal and dielectric) [1]. Surface plasmons have been extensively studied and found suitable for such applications as extraordinary optical transmission [2-4], bio-molecular sensing [5-6], drug discovery [7-8], surface plasmon interference lithography [9], and spectroscopic applications [10].

Maxwell's equations can be solved in a planar film to give the SP dispersion relationship:

$$k = \frac{\omega}{c}\sqrt{\varepsilon_{eff}} \tag{1}$$

Where k is the wave vector of the electromagnetic field propagating parallel to the interface, ω is the angular frequency of the incident field, and ε_{eff} is the effective dielectric constant given by:

$$\varepsilon_{eff} = \frac{\varepsilon_d \varepsilon_m}{\varepsilon_d + \varepsilon_m} \tag{2}$$

Where, ε_d and ε_m represent the dielectric constant of the dielectric and the metal, respectively.

As formula (1) suggests, the angular momentum of the SP is greater than the free space momentum of the incident photon and thus exciting SP at the metal-dielectric interface requires special care. From equations (1) and (2) one can see that the surface plasmon resonance (SPR) condition is affected by modification of ε_d. The properties of the dielectric at the metal-dielectric interface are highly sensitive to the presence of adsorbates, which is the basis of the application of SP and SPR in chemical and bio-molecular sensing [11].

One method that has been used to visualize surface plasmons in nano-devices is apertureless near-field optical microscopy (a-NSOM) [12-13]. In apertureless NSOM, a small tip, usually an atomic force microscope (AFM) tip, is scanned across the surface of the device while vibrating in tapping mode. The end of this tip acts like

Novel Optical Systems Design and Optimization XIII, edited by G. Groot Gregory, R. John Koshel,
Proc. of SPIE Vol. 7787, 77870R · © 2010 SPIE · CCC code: 0277-786X/10/$18 · doi: 10.1117/12.861582

a sphere that couples to SPs generated by the near field of the device. The induced charge in the tip creates a field (dipole moment) which is measured by the detector [14-15].

Used for the source of infrared light in reference [12] above is a quantum cascade laser (QCL). QCL is a unipolar semiconductor laser and was first demonstrated [16] in 1994. It works on the principle of intersubband transition and shows watt level performance at room temperature [17]. Due to these properties and improvements over the last decade a fully integrated mid-wave infrared (MWIR) optical antenna integrated QCL was developed, showing strong near field localization [18-20].

Optical antennas have previously been explored in the visible region [21]. Optical antennas are similar to radio frequency (RF) antennas in that they are resonant structures that respond to specific wavelengths through the geometrical and material characteristics of the antenna as well as the surrounding environment. Though both RF and optical antennas have the same fundamental goal of controlling radiation patterns, there exists an underlying discrepancy. While RF antennas focus on optimization of far-field characteristics in order to obtain better transmission and reception performance, optical antennas emphasize the near field behavior to for example create a spot size that is smaller than the wavelength of incoming light.

It has already been said that a-NSOM typically uses an AFM in tapping mode to scan the surface of a device. Typically the way this works is that there is a small tip at the end of a long cantilever that is vibrating slightly above the resonant frequency of the cantilever while scanning the surface [22]. A laser beam is reflected off the back of the cantilever onto a quad detector and the amplitude and phase of vibration of the beam, and therefore the cantilever, are measured. Surface interaction forces such as the electrostatic force and the van der Waals force make the tip have some interaction with the surface even though it is not in contact with the surface [23]. Because the tip is vibrating slightly above resonant frequency the fundamental forces acting on the tip are out of phase with each other which lowers the amplitude and keeps the tip in non-contact mode [24]. The amplitude of vibration is fed into a feedback loop and a piezo and servo keep the tip out of contact with the surface of the sample as it scans.

The final piece of an a-NSOM setup and indeed many experimental setups is a lock-in amplifier. A lock-in amplifier basically measures the amplitude of a sinusoidal voltage. What makes a lock-in amplifier different than using the "measure amplitude" function of an oscilloscope, however, is that it can measure the amplitude of a sinusoid that is only one small component of a signal that contains a much broader frequency spectrum. A lock-in amplifier works on the principle of phase sensitive detection (PSD), which is basically a multiplier that multiplies the input signal with a reference signal. At the output of the PSD is a DC component giving the amplitude of the input signal, and higher harmonics. The output of the PSD is then low-pass filtered to get the final output [25].

2. SETUP

The experimental setup is pictured in Fig. 1, based on reference [26]. It can be explained from the point of view of the path light takes once it is generated in the laser. The I-V characteristic and spectrum of the antenna integrated with QCL is shown in Fig. 2. After light is generated in the QCL, it leaves the front facet and is focused by the nano-antenna which has been patterned on the front facet using focused ion beam (FIB) milling. An example of the nano-antenna is pictured in Fig. 3. We have patterned two kinds of antenna, a single nanorod antenna and a coupled nanorod antenna with a resonant length of ~2 μm. After it is focused by the nano-antenna, it interacts with the tip as described in the introduction and is modulated at the frequency of vibration of the AFM tip and couples back into the front facet of the laser.

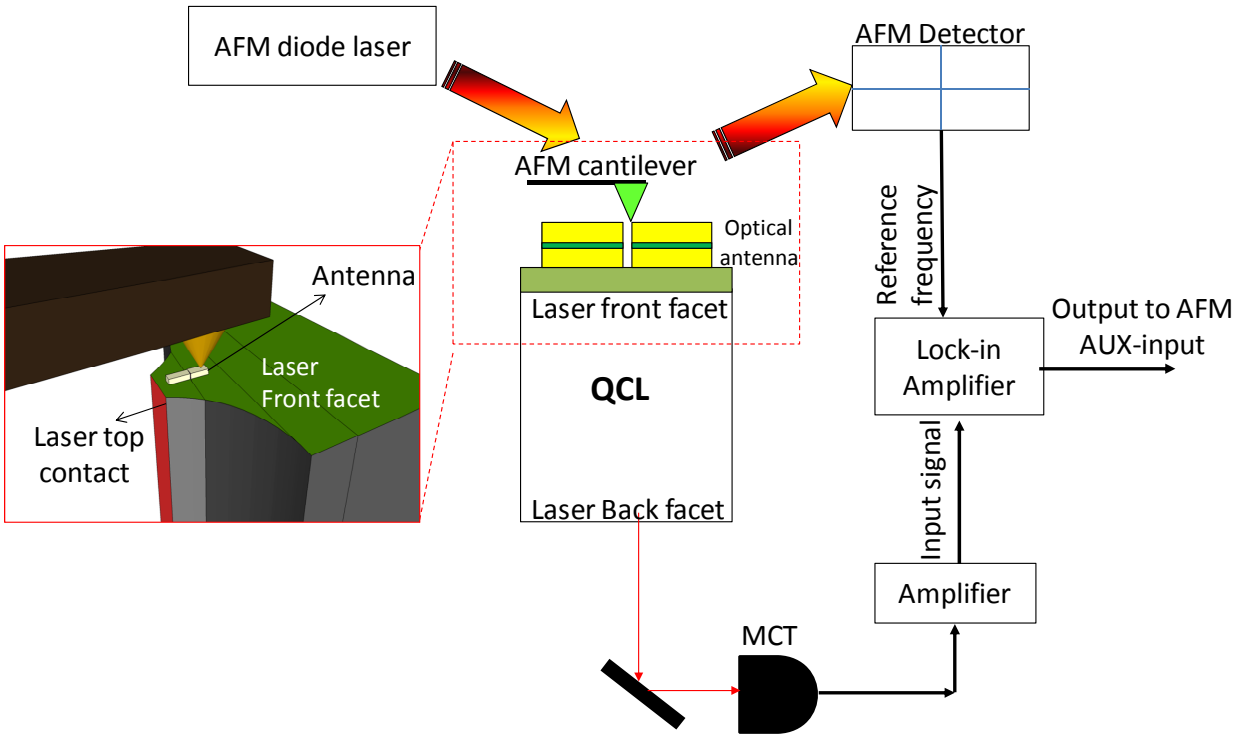

Figure 1 - Experimental setup.

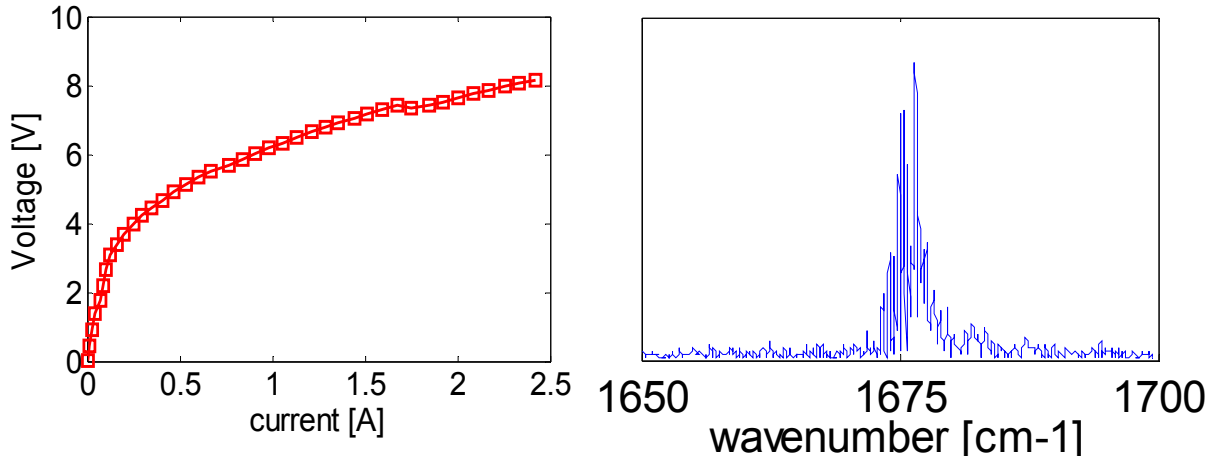

Figure 2 - (Left) I-V characteristic of the tested device. (Right) Spectrum of the antenna integrated laser.

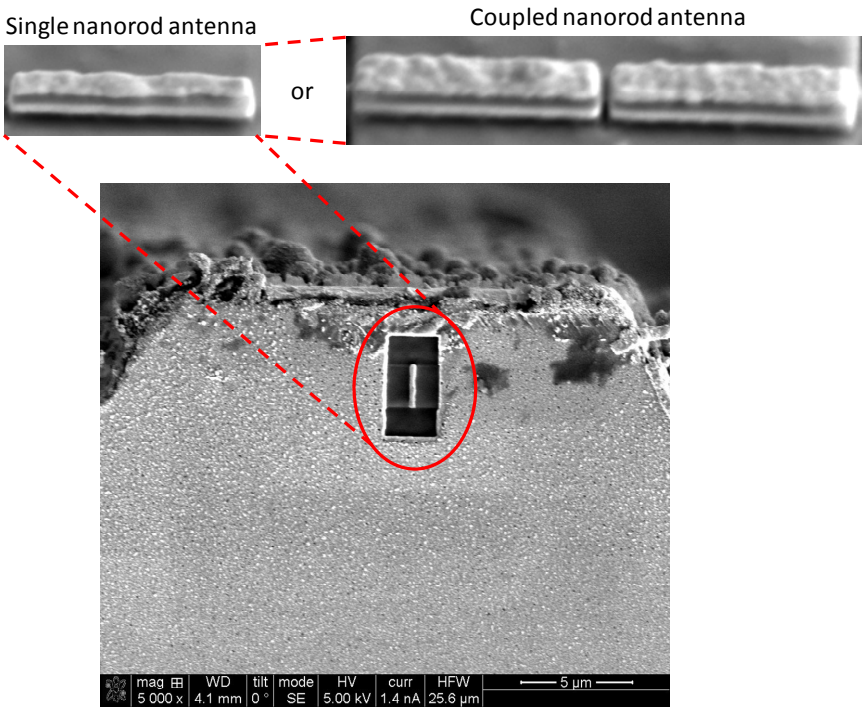

Figure 3 - Front facet of a QCL with patterned single nanorod antenna, also shown is a close up of a coupled nanorod antenna.

The light, now modulated by the frequency of the AFM tip, travels back through the gain medium of the laser, and is emitted from the back facet. It reflects off of a zinc-selenide beam splitter and is incident upon a mercury-cadmium-telluride (MCT) detector, which is sensitive in the mid to long-wave infrared. The detection spectrum of the MCT detector is shown in Fig. 4.

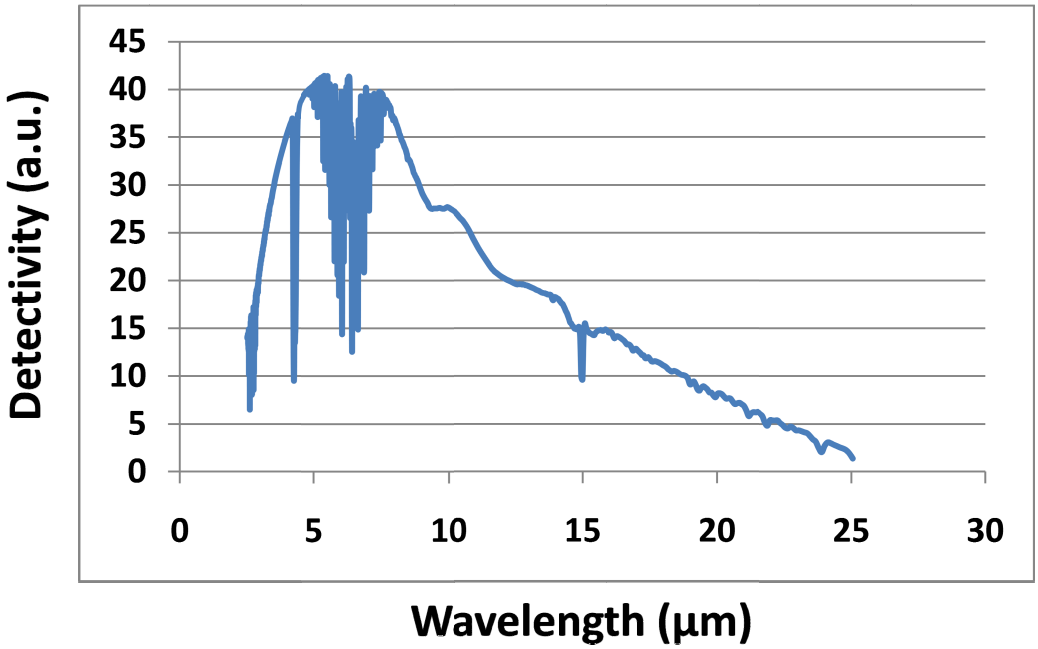

Figure 4 - Detection spectrum of the MCT detector used in the setup.

The signal from the MCT detector is then amplified with a low noise amplifier and sent to the lock-in amplifier.

Meanwhile, the lock-in amplifier has been fed the reference signal from the quad detector of the AFM. So the output of the lock-in gives the amplitude of the voltage of the MCT signal at the frequency of modulation of the AFM tip. This signal is sent to the auxiliary input of our AFM controller, which maps this signal to the position of the tip on the laser facet.

It should also be noted that we have two optical microscopes connected to this setup, one is looking down at the AFM tip from above and one is receiving the light from below the laser facet via beamsplitter to the MCT. The optical images from above and below the facet are pictured in Fig. 5.

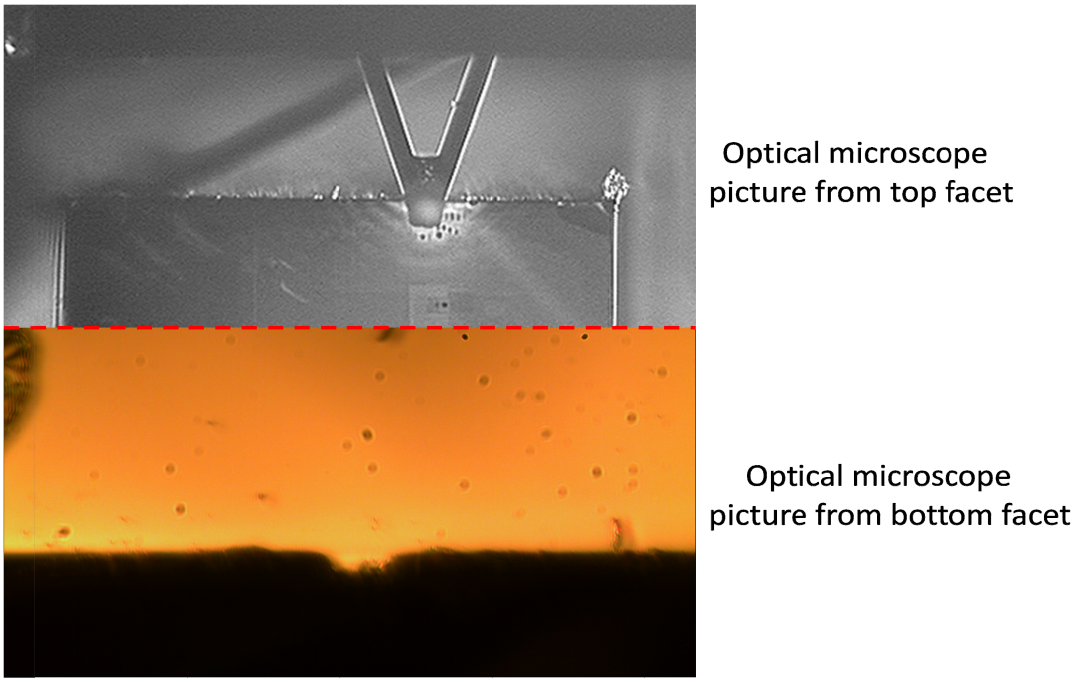

Figure 5 - Optical microscope images from the top and bottom facets of the laser.

3. RESULTS

We have performed a-NSOM on a single metal-dielectric-metal (MDM) nanorod antenna and a coupled MDM nanorod antenna and also simulated the structures with commercially available finite difference time-domain (FDTD) software, Lumerical. We have used the simulations to optimize the antenna structure and length. The results for the single nanorod antenna are shown in Fig. 6.

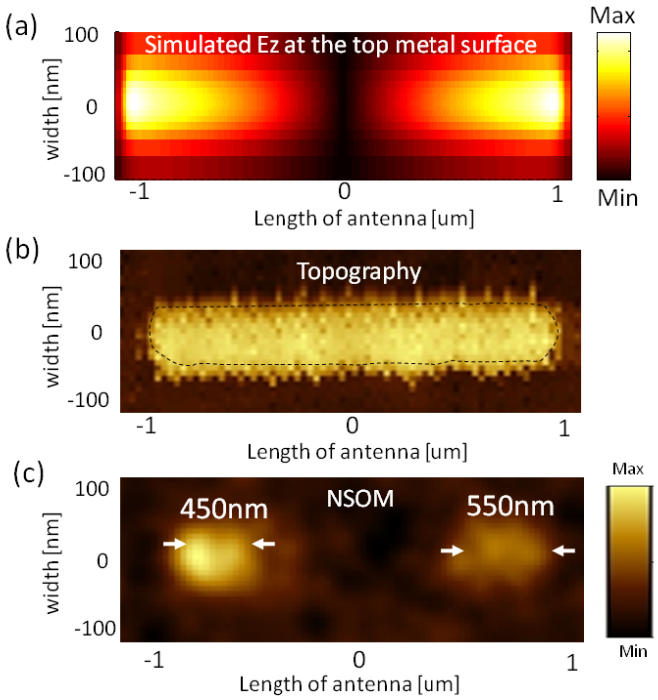

Figure 6 - (a) Simulated Ez on the top of the MDM nanorod. (b) AFM topography scan. (c) a-NSOM scan

We have found a more intense spot on the left hand side of the single MDM nanorod compared to the right. A similar observation has been reported in reference [27] and it is due to unsuppressed background noise. The experimental results are also consistent with the simulation results, showing a sub-wavelength spot at each end.

The results for the coupled MDM nanorod antenna are shown in Fig. 7. In the topography, you cannot see the slit between the two nanorods, because it is very narrow, only 50 nm. Also, the results agree with simulation and previous experiment, showing only two spots [28].

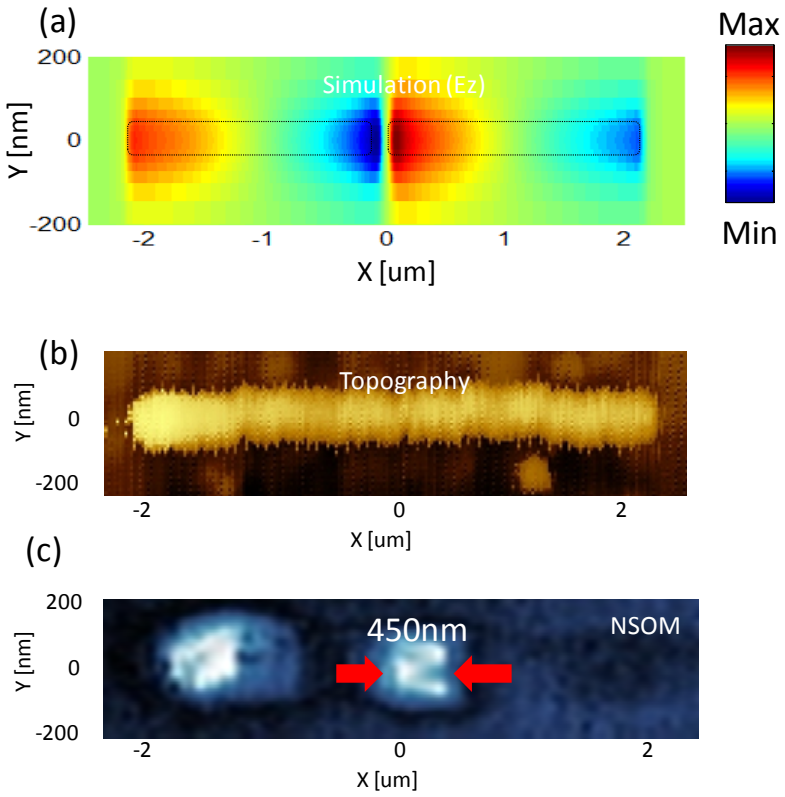

Figure 7 - (a) Simulated Ez for coupled MDM nanorod. (b) Topography for coupled MDM nanorod. (c) a-NSOM image showing the near field.

4. DISCUSSION

There are a few issues which should be noted to proceed with the above outlined experiment. First, it is noted that the laser is operated at 1% duty cycle (100 kHz, 100 ns pulse width) in pulsed mode. This can be very close to the resonance frequency of the AFM tip which can be anywhere from 20-300 kHz. If the frequencies are very close to each other it can produce a very noticeable beating effect of the NSOM signal. In the simplest case, one can have:

$$\sin(f_1 t) + \sin(f_2 t) = 2\cos\left(\frac{f_1 - f_2}{2} t\right)\sin\left(\frac{f_1 + f_2}{2} t\right) \quad (3)$$

Second, it should be noted that the radius of curvature of the AFM tip is important. It provides both the interaction strength with the surface as well as the resolution of the measurement. So, while one would prefer a

larger radius tip for a strong interaction, one would prefer not to have too large of a radius so as to limit the resolution of the measurement. The radius of curvature of the tips used the in the above experiments is on the order of 100 nm.

Lastly, as is the case with all AFM systems, the entire system is very dependent on vibration and temperature. The system should therefore be vibrationally and temperature isolated. We have found that over the time period of a scan it is more important to keep the system enclosed to reduce air currents than to keep the system completely temperature controlled. For vibrational isolation an optical table or AFM isolating setup should suffice.

5. CONCLUSION

Finally, it is important to note that there are other types of NSOM. First, there is aperture-probe NSOM, in which a tip containing a small aperture is scanned across the sample. Light is pushed through the aperture and collected with special lenses or mirrors after interacting with the sample [29].

Secondly, there is scattering-NSOM or s-NSOM in which the scattered signal is measured as opposed to the reflected signal. Thus, the sample can be illuminated from the top with an external laser and the scattered signal from the AFM tip is measured, again using mirrors or lenses to collect the scattered light [30].

Lastly, there is the type of integrated a-NSOM described in this paper. Having an integrated laser source can be a big advantage because it reduces the overall size and necessary optics required for the system to work. However, there are still electronics required to get the QCL to run in the first place, even though it is small, and an integrated laser may not always be desired. In conclusion, this is one type of NSOM, and its results have been confirmed by simulation and other types of NSOM.

6. REFERENCES

[1] H. Raether, *Surface plasmons on smooth and rough surfaces and on gratings*. New York: Springer, 1988.

[2] T. W. Ebbesen*, et al.*, "Extraordinary optical transmission through sub-wavelength hole arrays," *Nature,* vol. 391, pp. 667-669, Feb 1998.

[3] A. Lesuffleur*, et al.*, "Periodic nanohole arrays with shape-enhanced plasmon resonance as real-time biosensors," *Applied Physics Letters,* vol. 90, Jun 2007.

[4] Y. Liu*, et al.*, "Biosensing based upon molecular confinement in metallic nanocavity arrays," *Nanotechnology,* vol. 15, pp. 1368-1374, Sep 2004.

[5] C. T. Campbell and G. Kim, "SPR microscopy and its applications to high-throughput analyses of biomolecular binding events and their kinetics," *Biomaterials,* vol. 28, pp. 2380-2392, May 2007.

[6] S. M. Nie and S. R. Emery, "Probing single molecules and single nanoparticles by surface-enhanced Raman scattering," *Science,* vol. 275, pp. 1102-1106, Feb 1997.

[7] B. Liedberg*, et al.*, "SURFACE-PLASMON RESONANCE FOR GAS-DETECTION AND BIOSENSING," *Sensors and Actuators,* vol. 4, pp. 299-304, 1983.

[8] M. A. Cooper, "Optical biosensors in drug discovery," *Nature Reviews Drug Discovery,* vol. 1, pp. 515-528, Jul 2002.

[9] Z. W. Liu*, et al.*, "Focusing surface plasmons with a plasmonic lens," *Nano Letters,* vol. 5, pp. 1726-1729, Sep 2005.

[10] K. Kneipp*, et al.*, "Single molecule detection using surface-enhanced Raman scattering (SERS)," *Physical Review Letters,* vol. 78, pp. 1667-1670, Mar 1997.

[11] J. Homola, "Surface plasmon resonance sensors for detection of chemical and biological species," *Chemical Reviews,* vol. 108, pp. 462-493, Feb 2008.

[12] N. Yu*, et al.*, "Plasmonic quantum cascade laser antenna," *Applied Physics Letters,* vol. 91, Oct 2007.

[13] A. Cvitkovic*, et al.*, "Infrared imaging of single nanoparticles via strong field enhancement in a scanning nanogap," *Physical Review Letters,* vol. 97, Aug 2006.

[14] B. Knoll and F. Keilmann, "Enhanced dielectric contrast in scattering-type scanning near-field optical microscopy," *Optics Communications,* vol. 182, pp. 321-328, Aug 2000.
[15] R. Hillenbrand*, et al.*, "Pure optical contrast in scattering-type scanning near-field microscopy," *Journal of Microscopy-Oxford,* vol. 202, pp. 77-83, Apr 2001.
[16] J. Faist*, et al.*, "QUANTUM CASCADE LASER," *Science,* vol. 264, pp. 553-556, Apr 1994.
[17] Y. Bai*, et al.*, "Room temperature continuous wave operation of quantum cascade lasers with 12.5% wall plug efficiency," *Applied Physics Letters,* vol. 93, Jul 2008.
[18] E. Cubukcu*, et al.*, "Plasmonic laser antenna," *Applied Physics Letters,* vol. 89, Aug 2006.
[19] N. F. Yu*, et al.*, "Bowtie plasmonic quantum cascade laser antenna," *Optics Express,* vol. 15, pp. 13272-13281, Oct 2007.
[20] N. Yu*, et al.*, "Quantum cascade lasers with integrated plasmonic antenna-array collimators," *Optics Express,* vol. 16, pp. 19447-19461, Nov 2008.
[21] R. D. Grober*, et al.*, "Optical antenna: Towards a unity efficiency near-field optical probe," *Applied Physics Letters,* vol. 70, pp. 1354-1356, Mar 1997.
[22] G. Haugstad and R. R. Jones, "Mechanisms of dynamic force microscopy on polyvinyl alcohol: region-specific non-contact and intermittent contact regimes," *Ultramicroscopy,* vol. 76, pp. 77-86, Feb 1999.
[23] J. N. Israelachvili, *Intermolecular and Surface Forces*. London: Academic, 1992.
[24] J. Kohoutek*, et al.*, "Dynamic measurement and modeling of the Casimir force at the nanometer scale," *Applied Physics Letters,* vol. 96, Feb 2010.
[25] J. H. Scofield, "FREQUENCY-DOMAIN DESCRIPTION OF A LOCK-IN AMPLIFIER," *American Journal of Physics,* vol. 62, pp. 129-133, Feb 1994.
[26] E. Cubukcu*, et al.*, "Plasmonic Laser Antennas and Related Devices," *Ieee Journal of Selected Topics in Quantum Electronics,* vol. 14, pp. 1448-1461, Nov-Dec 2008.
[27] M. Schnell*, et al.*, "Amplitude- and Phase-Resolved Near-Field Mapping of Infrared Antenna Modes by Transmission-Mode Scattering-Type Near-Field Microscopy," *Journal of Physical Chemistry C,* vol. 114, pp. 7341-7345, Apr 2010.
[28] M. Schnell*, et al.*, "Controlling the near-field oscillations of loaded plasmonic nanoantennas," *Nature Photonics,* vol. 3, pp. 287-291, May 2009.
[29] B. Hecht*, et al.*, "Scanning near-field optical microscopy with aperture probes: Fundamentals and applications," *Journal of Chemical Physics,* vol. 112, pp. 7761-7774, May 2000.
[30] N. Ocelic*, et al.*, "Pseudoheterodyne detection for background-free near-field spectroscopy," *Applied Physics Letters,* vol. 89, Sep 2006.